Lattice dynamics of the ethylene crystal with interaction potentials from *ab initio* calculations

T. Wasiutynski,[a] A. van der Avoird, and R. M. Berns

Institute of Theoretical Chemistry, University of Nijmegen, Toernooiveld, Nijmegen, The Netherlands
(Received 18 May 1978)

The long range (electrostatic, dispersion, induction) and short range (exchange and penetration) interaction energy between ethylene molecules has been calculated by *ab initio* methods as a function of the molecular orientations and distances. The results, when fitted with an exp-6-1 atom–atom potential and used in a harmonic lattice dynamics calculation on the ethylene crystal, yield fair agreement with the experimental structure data, ir and Raman phonon frequencies. Although the fit with the atom–atom potential is reasonably good, some specific deviations from the *ab initio* results indicate the importance of the effects of chemical bonding on the intermolecular potential (leading to noncentral and nonpairwise additive atom–atom forces). The usual empirical atom–atom potentials are grossly corroborated, their main defect being the neglect or underestimate of electrostatic (quadrupole–quadrupole) interactions.

I. INTRODUCTION

Practically all calculations to date on the lattice stability and dynamics of molecular crystals have used simple empirical expressions for the interaction potential between the molecules. Very popular, for instance, is the use of so called atom–atom potentials[1] of the Lennard–Jones (12-6) or Buckingham (exp-6) type. The parameters occurring in these potentials are derived from experimentally known crystal data, such as the structure, the cohesion energy, the elastic constants,[2–4] or sometimes they are obtained by fitting the calculated lattice frequencies to measured ir and Raman spectra[5] or to phonon dispersion curves from inelastic neutron scattering.[6]

It is not certain that these empirical potentials correspond with the "real" interaction potential between the molecules, first of all, because the atom–atom potential model still lacks a sound physical basis and has never been thoroughly tested[7] and, secondly, because the crystal properties may not be equally sensitive to all aspects of the interaction potential. Some interactions, the electrostatic forces for example, may to some extent average out in the crystal[8] and it is typical that in many of the empirical potentials[1,2] these forces are left out completely, while the potentials still yield a reasonable description of several crystal properties.

For small, mostly diatomic molecules more detailed information about the interaction potential is becoming available, from beam scattering experiments,[9,10] relaxation measurements[11] and spectroscopic studies.[12,13] Only for the simplest case of the H_2 molecule, however, one has now rather good knowledge of the shape and the anisotropy of the interaction potential mainly as a result of *ab initio* calculations on the H_2–H_2[14–20] and H_2–He[19–25] interactions. Some of this information has already been used in lattice dynamics calculations on solid H_2.[26,27]

It is important to obtain similar information about the intermolecular interaction in the hydrocarbon crystals, in view of the various physically interesting effects displayed by these crystals. They have been subject of extensive semiempirical studies,[1–3,28–37] especially by Williams[2,3,28–30] who has been using atom–atom potentials with carefully optimized empirical parameters. Although Williams' calculated results show a nice quantitative agreement with the experimental properties considered (which have been used, for the main part, in the parameter fit), the remaining discrepancies[30] indicate already that the empirical atom–atom potentials must still be deficient in some respects.

Therefore, we thought it useful to perform an *ab initio* study of the interaction between ethylene molecules and to apply the results to a calculation of the structure and the dynamics of the ethylene crystal. This study is a continuation of earlier *ab initio* work on the ethylene dimer[8,38–40] and the crystal.[8] Thus, we can find out in how far the atom–atom potential model can be theoretically justified, how the empirical parameters compare with the theoretical results and which are the deficiencies of the model that must be corrected. On the other hand, since several experimental properties have been measured on solid ethylene, the crystal results provide a check on the accuracy of our *ab initio* calculations.

A similar study, concerning the static crystal properties, has recently been carried out for some hydrogen bonded systems.[41,42]

II. *AB INITIO* CALCULATIONS OF THE ETHYLENE-ETHYLENE INTERACTION

A. Procedure and results

Although our first calculation of the ethylene–ethylene interaction potential[38] was actually the most elegant one, since it yielded all short range (exchange and penetration) and long range (electrostatic, induction and dispersion) interactions in the single consistent formalism of the Multistructure Valence Bond method, further *ab initio* calculations[39,40] and some preliminary lattice dynamics studies have shown that the basis set employed originally was too small. As a result we had underestimated both the (first order) exchange repulsion and the (second order) induction and dispersion attractive interactions. Therefore, we have extended the basis and we have performed the calculation of the first order and second order interaction energy separately, for several intermolecular distances R and for several orientations, Ω_A and Ω_B, of the ethylene molecules in the dimer.

The first order energy, defined as:

$$\Delta E^{(1)}(R, \Omega_A, \Omega_B) = \langle \alpha \psi_0^A \psi_0^B | H^{AB} | \alpha \psi_0^A \psi_0^B \rangle$$
$$- \langle \psi_0^A | H^A | \psi_0^A \rangle - \langle \psi_0^B | H^B | \psi_0^B \rangle , \quad (1)$$

was calculated "exactly,"[43] which means that all occur-ring one- and two-electron integrals were accurately evaluated and that the result is valid at all distances. The ethylene monomer wave functions, ψ_0^A and ψ_0^B, were taken as ground state Hartree-Fock MO-LCAO wave-functions (Slater determinants), the operators H^{AB}, H^A and H^B are the dimer and monomer Hamiltonians, re-spectively, and α is the antisymmetrizer over the dimer (including normalization). For the expansion of the MO's a double-zeta basis of Gaussian type atomic orbit-als (basis B of Ref. 39) was used and sometimes,[44] for comparison, also a still more extended basis containing $3d$ orbitals on C and $2p$ on H (basis C of Ref. 39).

This first order energy comprises an electrostatic component, $\Delta E_{elec}^{(1)}$, which is obtained from expression (1) by substituting the identity operator for α, and a short-range exchange contribution, $\Delta E_{exch}^{(1)} \equiv \Delta E^{(1)} - \Delta E_{elec}^{(1)}$, arising from the antisymmetrization. For large distance the electrostatic energy can be approxi-mated by the multipole expansion:

$$\Delta E_{mult}^{(1)} = C_5(\Omega_A, \Omega_B)R^{-5} + C_7(\Omega_A, \Omega_B)R^{-7} + \cdots \quad (2)$$

and the deviation, $\Delta E_{elec}^{(1)} - \Delta E_{mult}^{(1)} = \Delta E_{pen}^{(1)}$, is due to the penetration between the charge clouds A and B, at short distance. The two leading terms in the multipole inter-action energy, $\Delta E_{mult}^{(1)}$, have been calculated in Refs. 8 and 39 for the same basis sets. All the first order re-sults have been collected in Tables I and II.

The second order energy was calculated in the multi-pole expansion, truncated after the two principal terms:

$$\Delta E^{(2)}(R, \Omega_A, \Omega_B) = - C_6(\Omega_A, \Omega_B)R^{-6} - C_8(\Omega_A, \Omega_B)R^{-8} \quad (3)$$

and the second order Rayleigh-Schrödinger perturba-tion expressions for the orientation dependent coeffi-cients C_6 and C_8 were also evaluated by ab initio calcu-lations. To this end, Mulder et al.[39,45] have used anoth-er basis set (D of Ref. 39), which is also an extension of basis B with $3d$ orbitals on C and $2p$'s on H with the purpose of providing a nearly complete set of virtual states in the second order expression.[39] As a check on this basis several completeness tests have been per-formed and the calculated molecular dipole polarizabil-ity of ethylene ($\alpha_{xx} = 26.5$ a. u., $\alpha_{yy} = 41.1$ a. u., $\alpha_{zz} = 23.2$ a. u.) agrees rather well with experiment[46,47] ($\alpha_{xx} = 26.1$ a. u., $\alpha_{yy} = 36.4$ a. u., $\alpha_{zz} = 23.0$ a. u.). Also the orientationally averaged C_6 plus C_8 contribution[40] is in good agreement with the experimental result from viscosity data.[48] The calculation of the separate contri-butions to $\Delta E^{(2)}$, i. e., the induction and the dispersion energy, for several conformations of the ethylene dimer is described in Refs. 8 and 39 and some results are listed in Table III.

B. Conclusions

Although we cannot be certain about the accuracy of the ab initio interaction energies listed in Tables I, II and III, we have tried to make some estimates of this accuracy.

The calculated molecular quadrupole moment, $Q_{2,0}$, agrees fairly well with the experimental value[49] and hardly changes when the AO basis set in the calculations is further extended. Also the different first order ener-gy contributions $\Delta E_{exch}^{(1)}$, $\Delta E_{elec}^{(1)}$, $\Delta E_{mult}^{(1)}$, $\Delta E_{pen}^{(1)}$ are prac-tically insensitive to basis set extension and so we ex-pect both the long range interaction, $\Delta E_{mult}^{(1)}$, which is nearly equal to $\Delta E_{elec}^{(1)}$ for large R, and the "overlap" contributions $\Delta E_{exch}^{(1)}$ and $\Delta E_{pen}^{(1)}$ to be rather accurate. The main error in these first order results is caused by the ne-glect of the intramolecular electron correlation and, on the basis of experience with smaller molecules, we es-timate this error to be not larger than 10% of the inter-action energy in the whole region of interest.

The same agreement with the scarce experimental quantities available is found for the second order prop-erties: the dipole polarizability[39] and the isotropic C_6 value.[40] Also it was checked that the second order re-sults are practically "saturated" with respect to basis set extension. In contrast with the first order energy, however, which was evaluated exactly, the second order energy was calculated in the multipole expansion only. This implies the neglect of charge overlap effects so that, formally, the results are just valid for large dis-tances. Moreover, the multipole expansion was trun-cated after the first two terms, while we found[39] that this expansion converges rather slowly for short dis-tances. The resulting errors must cancel to some ex-tent, though, and we estimate on the basis of previous studies[8,39,40] that the maximum error in the second en-ergy, which occurs for the nearest neighbor contacts in the ethylene crystal, is still not larger than about 20%.

As we have indicated in Table III, the induction energy is only a very small fraction of the total second order interaction, so that it can be neglected with respect to the dispersion energy.

III. ANALYTIC FIT BY ATOM-ATOM POTENTIALS

A. Fitting procedure and results

Since the atom-atom potential model has been exten-sively applied (with empirical parameters) and since it is rather convenient for lattice dynamics calculations, we have chosen this model to fit our ab initio calculated interaction potential between two ethylene molecules. The interaction energy between two molecules, A and B, is written as:

$$\Delta E_{AB} = \sum_i^A \sum_j^B V_{ij} \quad (4)$$

with

$$V_{ij}(r_{ij}) = q_i q_j r_{ij}^{-1} - A_{ij} r_{ij}^{-6} + B_{ij} \exp(-C_{ij} r_{ij}) , \quad (5)$$

where the first term in V_{ij} should account for the elec-trostatic energy between two atoms with net charges q_i and q_j at a distance r_{ij}, the second term for the long range attractive interactions and the last term for the short range repulsions. At first, we have tried to fit the total first plus second order interaction energy by adapting all parameters at once, but as there is a high degree of correlation between the fit parameters we have used the following procedure.

TABLE I. Electrostatic energy.

Dimer geometry[a] Ω_A, Ω_B	R(bohr)	$\Delta E_{elec.}^{(1)}$ [b] (kcal/mole)	$\Delta E_{mult.}^{(1)}$ [b] (kcal/mole)	$\Delta E_{fit:\bigcirc}$ [c] (kcal/mole)	$\Delta E_{fit\bigcirc}$ [d,e] (kcal/mole)
I	7	0.5226	0.4959	0.9799	0.8990
	8	0.5008	0.3953	0.5534	0.5221
	10	0.2085	0.1882	0.2049	0.2009
	12	...	0.0857	0.0884	0.0888
	15	...	0.0312	0.0308	0.0316
	20	...	0.0080	0.0077	0.0080
II[f]	7	0.2434	0.4729	0.5119	0.4791
	8	0.2963	0.2932	0.3224	0.3060
	10	0.1439	0.1324	0.1394	0.1358
	12	...	0.0657	0.0665	0.0661
	15	...	0.0259	0.0254	0.0258
	20	...	0.0072	0.0068	0.0071
III	7	−3.1958	−0.1552	−0.3067	−0.4402
	8	−0.6170	−0.1639	−0.2074	−0.2934
	9	−0.1851(−0.1907)	−0.1230	−0.1364	−0.1920
	10	−0.0964(−0.0997)	−0.0861	−0.0902	−0.1268
	12	...	−0.0417	−0.0417	−0.0585
	15	...	−0.0156	−0.0152	−0.0214
	20	...	−0.0040	−0.0039	−0.0055
IV	7	−3.7029	−0.2056	−0.3865	−0.4887
	8	−0.6986	−0.1829	−0.2335	−0.2918
	10	−0.1033	−0.0898	−0.0938	−0.1182
	12	...	−0.0426	−0.0422	−0.0538
	15	...	−0.0157	−0.0152	−0.0196
	20	...	−0.0041	−0.0039	−0.0051
V	7	−3.4614	0.5866	1.0211	1.3843
	8	−0.2050	0.3056	0.4241	0.5392
	10	0.1176	0.1019	0.1119	0.1266
	12	...	0.0414	0.0413	0.0437
	15	...	0.0137	0.0130	0.0131
	20	...	0.0033	0.0030	0.0030
VI	7	−3.2847	−0.6615	−0.6123	−0.8981
	8	−0.6359	−0.2347	−0.2266	−0.3653
	10	−0.0461	−0.0366	−0.0367	−0.0711
	12	...	−0.0059	−0.0062	−0.0166
	15	...	0.0004	0.0003	−0.0021
	20	...	0.0006	0.0005	0.0001
VII	7	...	0.7039	1.3373	2.6724
	8	−2.7724	0.3535	0.5116	0.9006
	9	−0.1688	0.1933	0.2370	0.3842
	12	...	0.0447	0.0452	0.0668
	15	...	0.0145	0.0140	0.0204
	20	...	0.0034	0.0032	0.0047
XII	7	...	−0.0231	−0.3060	−0.0553
	8	...	−0.1067	−0.1898	−0.0520
	10	...	−0.0715	−0.0789	−0.0318
	12	...	−0.0367	−0.0363	−0.0175
	15	...	−0.0142	−0.0133	−0.0073
	20	...	−0.0038	−0.0035	−0.0021
σ[g]		...	0.0	0.036	0.23

[a]The orientations (Ω_A, Ω_B) of the molecules numbered by the Roman figures are indicated schematically in Fig. 2.

[b]From *ab initio* calculations; definitions, see the text. The GTO basis used is: C(9,5/4,2), H(4/2) (Ref. 39, basis B), for the results in parentheses: C(9,5, 1/4, 2,1), H(4,1/2,1) (Ref. 39, basis C).

[c]Atom−atom fit with the point charges shifted from the nuclei, see Fig. 1. This fit was made for the distances $R = 12, 13, 14, 15, 16, 18, 20, 22$ bohr.

[d]Atom−atom fit with the point charges on the nuclei. The same distances were used in the fit as in c).

[e]The empirical atom−atom potential ② from Ref. 29 yields an electrostatic energy which differs from this fit by exactly a factor of 0.37. This leads to a root mean square deviation

TABLE I (*Continued*)

$\sigma = 0.62$ with respect to $\Delta E_{\text{mult}}^{(1)}$.

[f] For this orientation R is the distance between the two molecular planes.

[g] The root mean square relative deviation is defined as:

$$\sigma = \left[\frac{1}{N_R} \sum_R \frac{\sum_{\Omega_A, \Omega_B} (\Delta E_{\text{fit}} - \Delta E_{\text{mult}}^{(1)})^2}{\sum_{\Omega_A, \Omega_B} {\Delta E_{\text{mult}}^{(1)}}^2} \right]^{1/2} ,$$

where the summations run over all the orientations (Ω_A, Ω_B) in this table and the distances $R = 12 - 22$ bohr $(N_R = 8)$. The summation over the orientations was carried out before taking the ratios, since for some orientations the electrostatic energy is very close to zero.

TABLE II. Short range energy.

Dimer geometry[a]		$\Delta E^{(1)}$ [b]	$\Delta E_{\text{short range}}^{(1)}$ [c]	$\Delta E_{\text{fit}\bigcirc}$ [d]	$\Delta E_{\text{fit}\bigcirc}$ [e]	$\Delta E_{\text{empirical}\bigcirc}$ [f]	$\Delta E_{\text{empirical}\bigcirc}$ [g]
Ω_A, Ω_B	R(bohr)	(kcal/mole)	(kcal/mole)	(kcal/mole)	(kcal/mole)	(kcal/mole)	(kcal/mole)
I	7	2.4498	1.4699	1.4198	0.7830	0.4604	0.4435
	8	0.8685	0.3151	0.2742	0.1495	0.0709	0.0685
	10	0.2182	0.0133	0.0101	0.0054	0.0017	0.0016
II [h]	7	1.4151	0.9032	0.9704	0.5552	0.3185	0.3148
	8	0.5199	0.1975	0.1919	0.1078	0.0501	0.0496
	10	0.1498	0.0104	0.0074	0.0040	0.0012	0.0012
III	7	7.1000	7.4066	6.6205	5.6981	4.4580	5.2510
	8	1.2387	1.4461	1.2806	1.0863	0.7173	0.8543
	9	0.1098 (0.1021)	0.2462	0.2454	0.2026	0.1126	0.1349
	10	−0.0555(−0.0588)	0.0347	0.0468	0.0373	0.0174	0.0209
IV	7	7.6388	8.0251	6.7170	6.6206	5.2915	6.5263
	8	1.2821	1.5155	1.2934	1.2059	0.8153	1.0032
	10	−0.0605	0.0333	0.0470	0.0394	0.0188	0.0230
V	7	17.3186	16.2972	15.4433	18.1144	21.9214	25.7024
	8	2.9360	2.5118	2.5771	3.0438	3.2852	3.8871
	10	0.1705	0.0586	0.0745	0.0858	0.0719	0.0861
VI	7	7.1250	7.7372	8.2481	10.0932	9.2440	11.6088
	8	0.6744	1.2963	1.6617	2.0217	1.7096	2.1391
	10	−0.0142	0.0225	0.0604	0.0699	0.0487	0.0605
VII	8	12.4209	11.9094	10.8979	12.2708	13.6009	16.0984
	9	1.9890	1.7521	1.8549	2.0806	2.0207	2.4152
	10.5	0.1902	0.0956	0.1340	0.1452	0.1145	0.1381
	11.5	0.0734	0.0164	0.0236	0.0247	0.0168	0.0203
VIII	8	7.8373	8.1044	8.0638	9.4368	8.8979	11.0085
	9	1.1378	1.2354	1.5248	1.7505	1.4834	1.8337
	10.5	0.0321	0.0548	0.1208	0.1320	0.0937	0.1155
	11.5	−0.0053	0.0028	0.0221	0.0231	0.0144	0.0177
σ [i]		$\cdots$	0.0	0.13	0.33	0.45	0.53

[a] The orientations (Ω_A, Ω_B) of the molecules are indicated schematically in Fig. 3.

[b] From *ab initio* calculations, basis B; results in parentheses with basis C (see Table I).

[c] Defined as: $\Delta E_{\text{short range}}^{(1)} = \Delta E^{(1)} - \Delta E_{\text{point charge}}^{(1)}$, where $\Delta E_{\text{point charge}}^{(1)}$ is the electrostatic energy from the best long range fit to the *ab initio* results in Table I, fit ①.

[d] Atom−atom fit to $\Delta E_{\text{short range}}^{(1)}$ (for the shortest two distances, R) as described in the text, but without averaging constraints for the C−H parameters.

[e] Same as[d] with averaging constraints for the C−H parameters.

[f] From Williams (Ref. 28).

[g] From Williams (Ref. 29).

[h] For this orientation R is the distance between the two molecular planes.

[i] The root mean square relative deviation:

$$\sigma = \left[\frac{1}{N} \sum_R \sum_{\Omega_A, \Omega_B} \frac{(\Delta E_{\text{fit}} - \Delta E_{\text{short range}}^{(1)})^2}{(\Delta E_{\text{short range}}^{(1)})^2} \right]^{1/2}$$

for the smallest two distances $(N = 16)$.

TABLE III. Dispersion energy.

Dimer geometry[a]		$\Delta E^{(2)}$ [b]	ΔE_{fit} [c]	$\Delta E_{empirical}$ ① [d]	$\Delta E_{empirical}$ ② [e]
Ω_A, Ω_B	R(bohr)	(kcal/mole)	(kcal/mole)	(kcal/mole)	(kcal/mole)
I	12	0.0782	0.0804	0.0626	0.0600
	15	0.0203	0.0219	0.0172	0.0166
	19	0.0049	0.0055	0.0043	0.0041
IX	12	0.1487	0.1457	0.1207	0.1226
	15	0.0348	0.0323	0.0264	0.0264
	19	0.0077	0.0070	0.0056	0.0056
III	12	0.1163	0.1160	0.0936	0.0926
	15	0.0280	0.0280	0.0225	0.0222
	19	0.0063	0.0064	0.0051	0.0050
X	12	0.1646	0.1686	0.1460	0.1542
	15	0.0378	0.0346	0.0289	0.0296
	19	0.0083	0.0072	0.0059	0.0059
V	12	0.1323	0.1332	0.1124	0.1162
	15	0.0314	0.0304	0.0252	0.0254
	19	0.0070	0.0067	0.0055	0.0055
XI	12	0.0826	0.0845	0.0669	0.0650
	15	0.0213	0.0227	0.0179	0.0175
	19	0.0051	0.0056	0.0045	0.0043
VII	12	0.1806	0.1857	0.1586	0.1656
	15	0.0415	0.0375	0.0311	0.0317
	19	0.0091	0.0076	0.0062	0.0062
XII	12	0.0888	0.0895	0.0720	0.0711
	15	0.0225	0.0235	0.0188	0.0185
	19	0.0053	0.0057	0.0046	0.0045
σ [f]		0.0	0.071	0.20	0.21

[a]The orientations Ω_A, Ω_B of the molecules are indicated schematically in Fig. 4.
[b]From *ab initio* calculations in the multipole expansion (see text) using the nonempirical mean energy approximation with basis set D (see Ref. 39, formulas 4 and 5). The induction energy is not tabulated since it is always smaller than the dispersion energy by a factor of 35 or more.
[c]Atom–atom fit for $R = 12, 13, \cdots, 19$ bohr as described in the text.
[d]From Williams (Ref. 28).
[e]From Williams (Ref. 29).
[f]The root mean square relative deviation σ is defined as in Table II, for $R = 12, 13, \cdots, 19$ bohr ($N = 64$).

(i) The first order electrostatic energy as calculated in the multipole expansion, $\Delta E^{(1)}_{mult}$, for several conformations for $R = 12.0$ to 22.0 a.u. (see Table I) is fitted by the term:

$$V^{el}_{ij} = q_i q_j r^{-1}_{ij} , \qquad (5a)$$

which contains the following fit parameters for every atom i: the charge q_i, and the coordinates (x_i, y_i) that fix the position of the charge i, which is displaced in the molecular plane with respect to the corresponding nucleus. (See Fig. 1.)

Altogether, because of symmetry and charge neutrality, this yields four independent fit parameters for the ethylene molecule.

A model with the charges centered on the nuclei contains only one independent parameter, which could be fitted to the main component $Q_{2,0}$ of the molecular quadrupole moment, for instance. Such a model could not correctly represent the electrostatic interaction as a function of the molecular orientations, however.[8] The fit to the electrostatic interaction is much improved by the present 4-parameter model with the shifted charges

(Table I, Fig. 2). A model with the charge centers displaced from the nuclei is also physically reasonable, since it reflects the effects of the chemical bonding.

We have chosen to fit only the long range part of the electrostatic energy, $\Delta E^{(1)}_{mult}$, which is nearly equal to $\Delta E^{(1)}_{elec}$ for large R, because for shorter distance the exactly calculated behavior of $\Delta E^{(1)}_{elec}$ could not be correctly represented by the point charge model. This is due to the penetration between the charge clouds: the deviation of $\Delta E^{(1)}_{point\ charge}$ from $\Delta E^{(1)}_{elec}$ begins to occur at the same distance as the deviation between $\Delta E^{(1)}_{elec}$ and $\Delta E^{(1)}_{mult}$. This penetration interaction is a short range effect, it has about the same distance dependence as $\Delta E^{(1)}_{exch}$, and so we have added the difference $(\Delta E^{(1)}_{elec} - \Delta E^{(1)}_{point\ charge})$ to the short range exchange repulsion, $\Delta E^{(1)}_{exch}$.[50] The sum of these two overlap contributions has been fitted with an exponential function (ii).

(ii) The short range interactions arising from penetration, $\Delta E^{(1)}_{elec} - \Delta E^{(1)}_{point\ charge}$, and from exchange, $\Delta E^{(1)}_{exch}$, have been fitted by:

$$V^{overlap}_{ij} = B_{ij} \exp(-C_{ij} r_{ij}) . \qquad (5b)$$

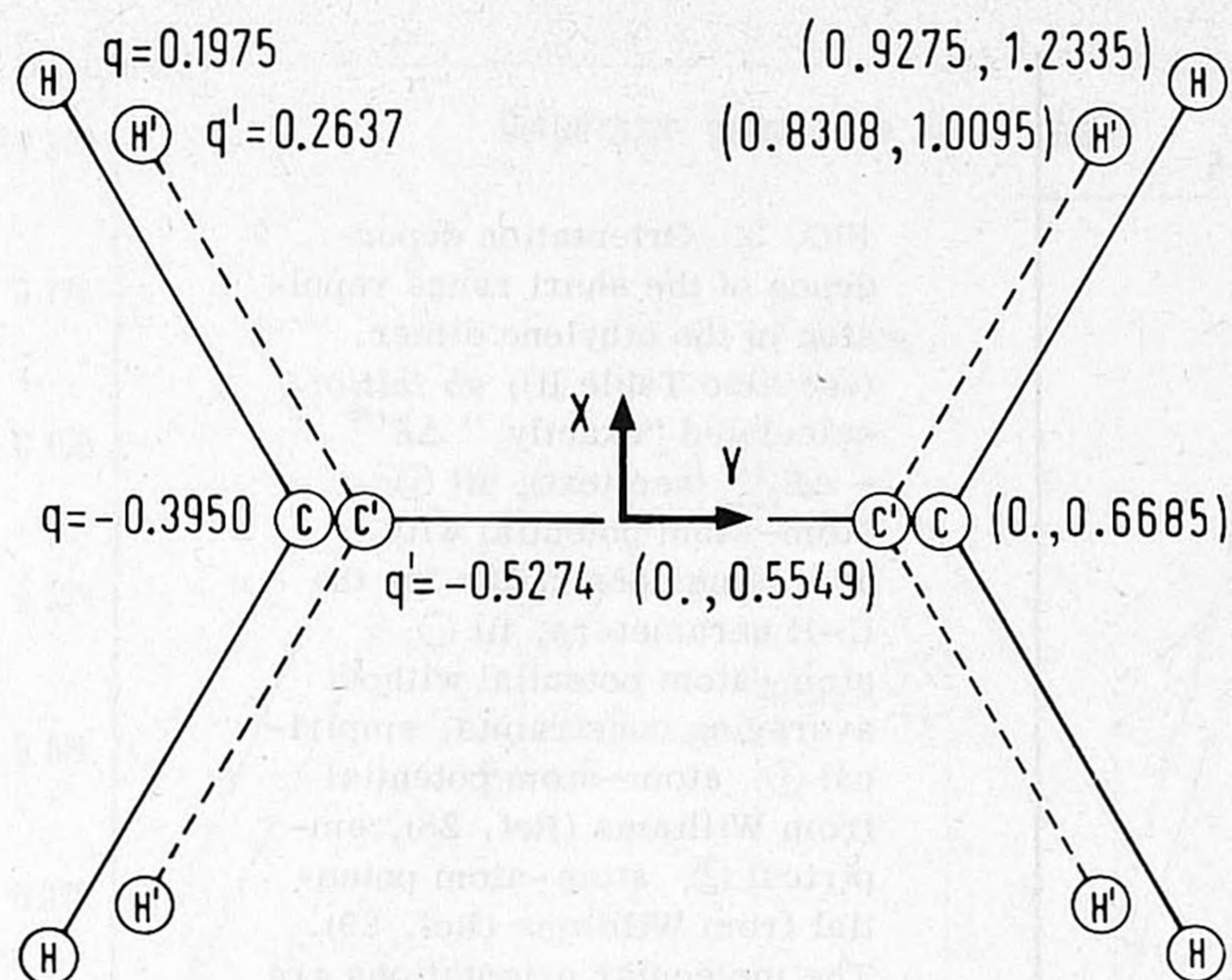FIG. 1. Point charges (in unit charges) and coordinates (in Å) in the ethylene molecule. The charges q' with positions $\widehat{C'}$ and $\widehat{H'}$, which are shifted with respect to the nuclei $\odot$ and $\odot$ are obtained from the best fit of the long range electrostatic interaction in the dimer (see Table I, Fig. 2). The charges q on the nuclei fix the main component of the molecular quadrupole moment, $Q_{2,0}$.

The present results and, even more so, our previous *ab initio* results for smaller systems[24,51,52] which have been calculated for a wider range of distances, show that the short range interactions indeed display a nearly exponential distance dependence.

In fitting the orientational dependence of the short range interactions we have met the following problem, however. If all the parameters B_{CC}, C_{CC}, B_{CH}, C_{CH}, B_{HH}, C_{HH} in the atom–atom potential of type (5b) were freely varied to obtain the best fit to the *ab initio* short range repulsion calculated for eight different orienta-

tions and two or three distances of the molecules in the ethylene dimer, we obtained several results with small numerical deviations but with quite unphysical interaction parameters. An example is shown by the fit ③ in Fig. 3 which has a much smaller mean square deviation (see Table II) from the *ab initio* results than the final fit described below. The carbon–hydrogen repulsion is absent in this fit ($B_{CH} = 0$), however, and its application to the lattice structure optimization and the phonon calculations yielded quite unrealistic results. We have tried, without success, to avoid this problem by taking a different form of the atom–atom repulsion, e.g., r^{-n}, or by shifting the atomic force centers away from the nuclei to the charge centers from fit (i).

We explain this problem as follows. The true interaction potential between the molecules does not have the atom–atom model potential form; it will include non-central forces between the atoms as well as nonadditive three-atom and higher interactions. This is illustrated by the results in Table II where we see, for instance, that the carbon–carbon repulsions, which are the ones with the longest range, actually have a smaller exponential decay for the geometries I and II than for other geometries. The exponent C_{CC}, if it were only fitted to the results of geometries I and II, would have a value 2.95 Å^{-1}. This particular effect is caused, we think, by the relatively diffuse carbon π-electron clouds. As a result of such effects there is probably a sizable deviation between any atom–atom model potential and the true potential. Fitting the potential parameters for a limited set of dimer geometries it may be possible to obtain smaller deviations but this will not give a better atom–atom potential (for arbitrary other geometries). Therefore, in using a restricted set of *ab initio* results, as we have done, one must be very careful in fitting.

We have used the following procedure: the hydrogen–hydrogen repulsion parameters, B_{HH} and C_{HH}, were ob-
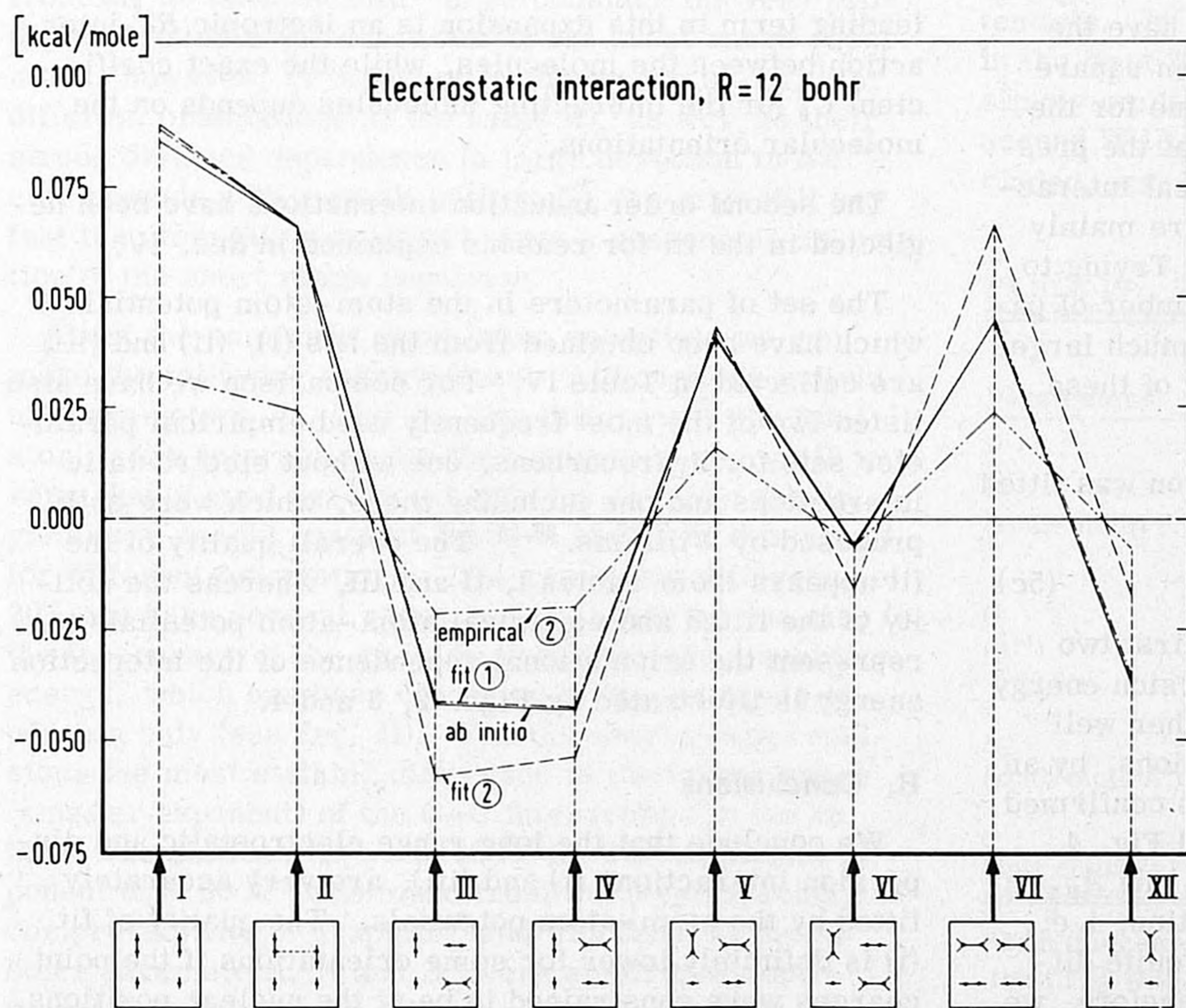

FIG. 2. Orientation dependence of the electrostatic interaction in the ethylene dimer (see also Table I); *ab initio*: calculated in the multipole expansion, $\Delta E^{(1)}_{mult.}$, fit ①: point charges shifted from the nuclei (see Fig. 1); fit ②: point charges on the nuclei; empirical ②: point charges from Williams (Ref. 29). The molecular orientations are indicated by giving two views of the dimer. For orientation II R is the distance between the molecular planes.
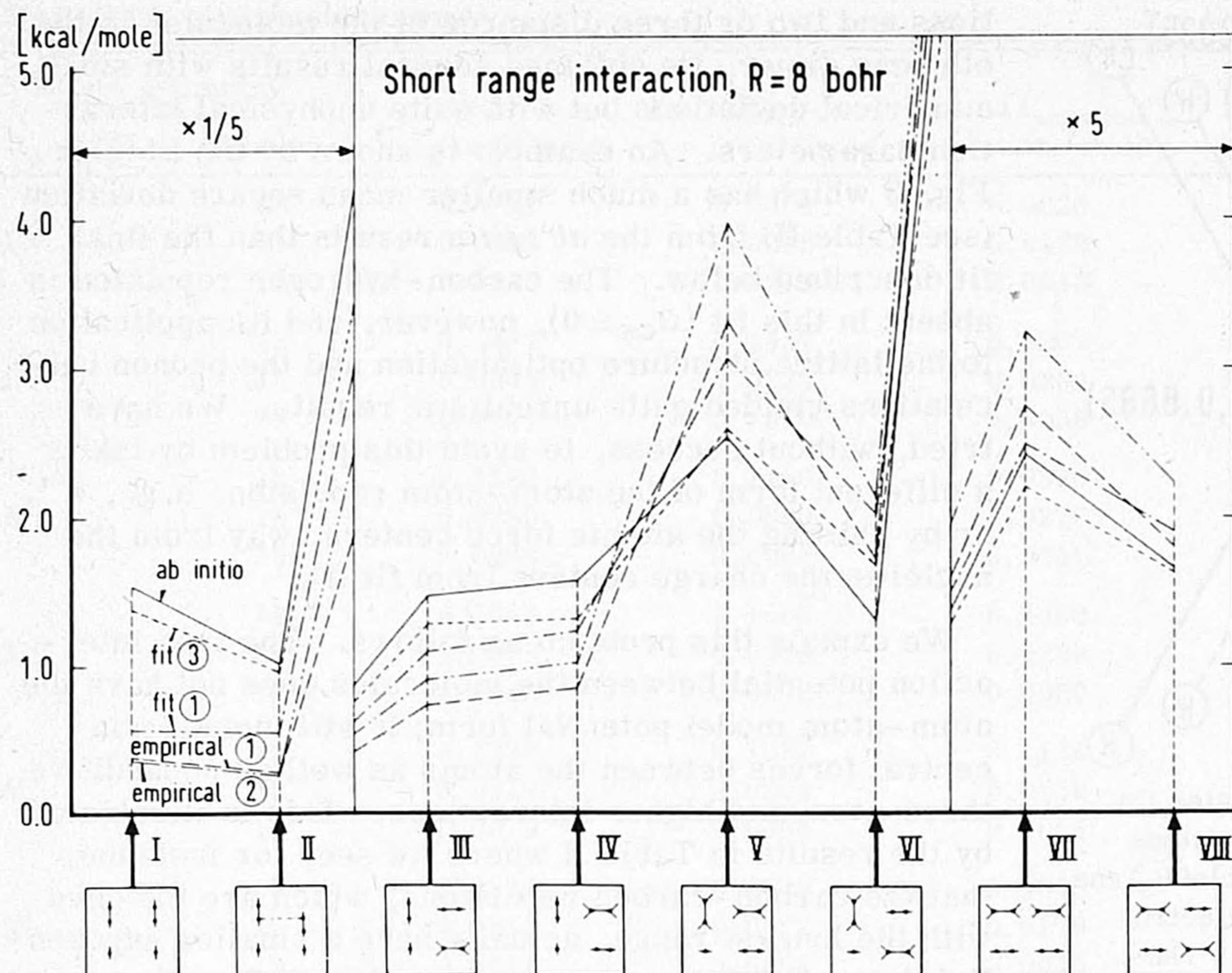
FIG. 3. Orientation dependence of the short range repulsion in the ethylene dimer. (see also Table II); *ab initio*: calculated "exactly," $\Delta E^{(1)} - \Delta E^{(1)}_{\text{p.c.}}$ (see text), fit ①: atom–atom potential with averaging constraints for the C–H parameters, fit ○: atom–atom potential without averaging constraints, empirical ①: atom–atom potential from Williams (Ref. 28), empirical ②: atom–atom potential from Williams (Ref. 29). The molecular orientations are indicated as in Fig. 2.

tained from the difference in interaction energy between geometries V and VI and from the difference between VII and VIII, which are both caused mainly by the hydrogen contacts. The agreement between these two results is good. Then we have fitted the carbon–carbon repulsion parameters (B_{CC} and C_{CC}) to the *ab initio* results for all orientations while the carbon–hydrogen parameters were constrained to be averages:

$$B_{CH} = (B_{CC} \cdot B_{HH})^{1/2}$$
$$C_{CH} = (C_{CC} + C_{HH})/2$$

and the hydrogen–hydrogen parameters were kept fixed. For this fit we have used the results at the shortest two distances where the *ab initio* results for the exchange and penetration interactions are expected to have the highest relative accuracy. Although the mean square deviation is considerably larger than the value for the best unrestricted parameter fit, we think that the present fit gives a better representation of the real interaction potential and that the resulting errors are mainly inherent to the atom–atom potential model. Trying to improve on this model would augment the number of parameters considerably and would require a much larger set of *ab initio* results to make a reliable fit of these parameters.

(iii) The second order dispersion attraction was fitted by an atom–atom potential:

$$V_{ij}^{\text{disp}} = -A_{ij} r_{ij}^{-6} . \tag{5c}$$

It has appeared already in Ref. (8) that the first two multipole terms $-C_6 R^{-6} - C_8 R^{-8}$ in the dispersion energy between two ethylene molecules could be rather well represented, for several molecular orientations, by an atom–atom potential of the r^{-6} type. This is confirmed by the present results shown in Table III and Fig. 4. If we choose the three parameters A_{CC}, A_{CH} and A_{HH} independently they show a rather high correlation, i.e., almost equally good fits can be obtained for quite different combinations of the parameters. Therefore, we

have applied the constraint $A_{CH} = (A_{CC} \cdot A_{HH})^{1/2}$ which can be justified by theoretical arguments and which has also been used in deriving most of the empirical parameter sets. This constraint hardly affects the quality of the fit and it gave much better defined values of the two independent parameters.

From the results in Table III it is evident that the fit between the atom–atom potential and the *ab initio* dispersion energy becomes worse for very large distances: the atom–atom interaction energy between the molecules is not sufficiently anisotropic for large R. This defect of the r^{-6} atom–atom potential is easily explained by making an expansion of the r^{-6} atom–atom interaction energy around the molecular centers of mass. The leading term in this expansion is an isotropic R^{-6} interaction between the molecules, while the exact coefficient C_6 for the interacting molecules depends on the molecular orientations.

The second order induction interactions have been neglected in the fit for reasons explained in Sec. IV.

The set of parameters in the atom–atom potential ① which have been obtained from the fits (i), (ii) and (iii) are collected in Table IV. For comparison we have also listed two of the most frequently used empirical parameter sets for hydrocarbons, one without electrostatic interactions and one including these, which were both proposed by Williams. [28,29] The overall quality of the fit appears from Tables I, II and III, whereas the ability of the fitted and empirical atom–atom potentials to represent the orientational dependence of the interaction energy is illustrated by Figs. 2, 3 and 4.

B. Conclusions

We conclude that the long range electrostatic and dispersion interactions (i) and (iii), are very accurately fitted by the atom–atom potentials. The quality of fit (i) is definitely lower for some orientations if the point charges were constrained to be at the nuclear positions.
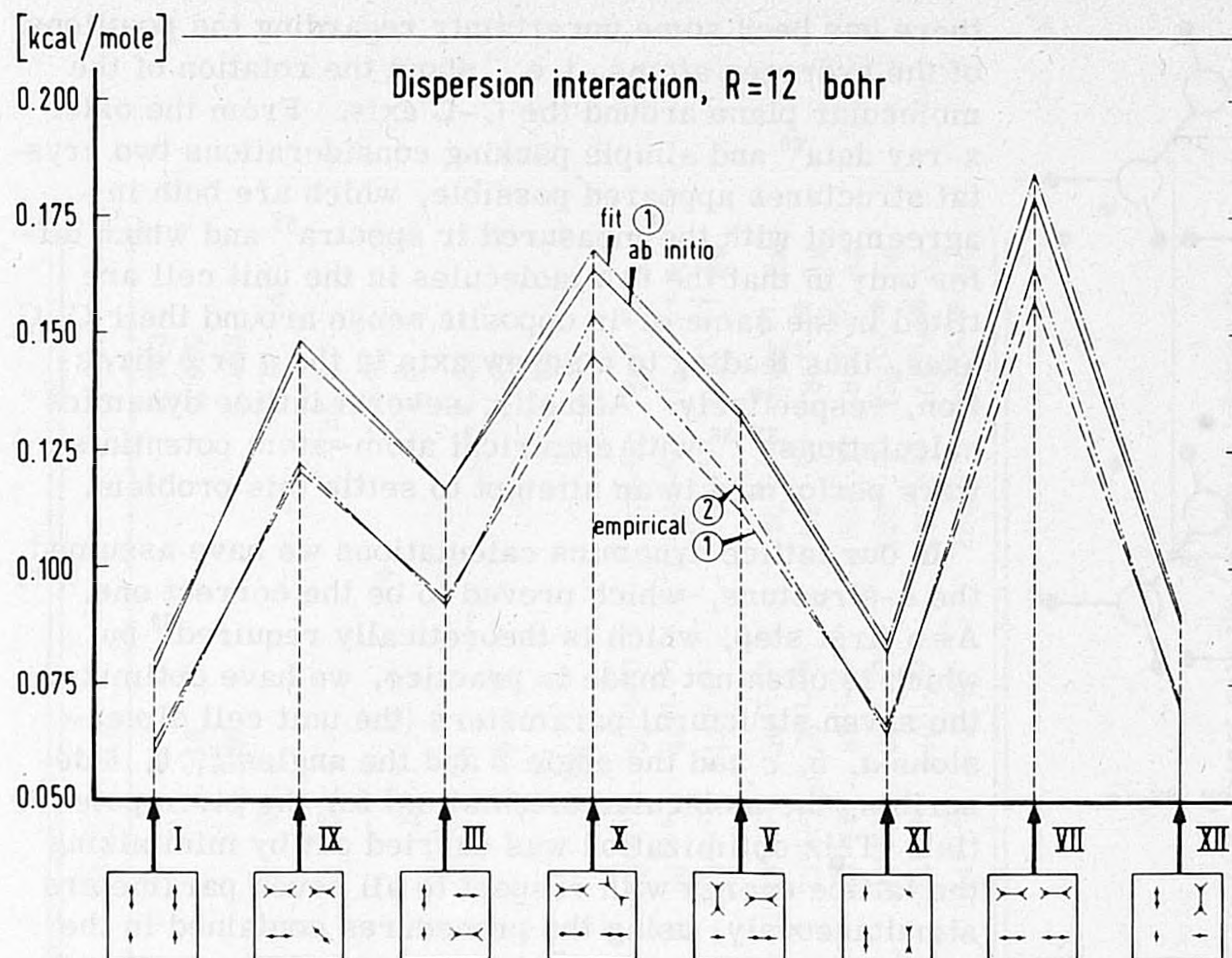
FIG. 4. Orientation dependence of the long range dispersion interactions in the ethylene dimer (see also Table III); *ab initio*: calculated in the multipole expansion, $\Delta E_{mult.}^{(2)}$, fit ①: atom–atom potential (with averaging constraint for the C–H parameter). Empirical ①. atom–atom potential from Williams (Ref. 28), empirical ②: atom–atom potential from Williams (Ref. 29). The molecular orientations are indicated as in Fig. 2.

The fit (iii) becomes slightly worse for very large R due to the incorrect asymptotic behavior of the r^{-6} atom–atom potential. The fit of the short range overlap repulsion (ii) shows a significantly larger mean square deviation than the long range fits. This must probably be assigned to the deviations of the exact intermolecular potential from a central atom–atom potential due to the effects of chemical bonding. Considering the large overlap between chemically bonding atoms the importance of such effects on the intermolecular overlap repulsion is not surprising.[53]

For some orientations (with relatively small repulsion) the atom–atom potential deviates by a factor of two from the *ab initio* result. If we consider the very pronounced anisotropic character of the short range repulsions, however, (a factor of 50 difference in ΔE^{AB} for different orientations at the same R), as well as their strong distance dependence (a large deviation in ΔE^{AB} corresponds with a small shift in R), we may still say that the atom–atom potential gives a reasonable description of the short range repulsion.

About the empirical atom–atom potentials we can make the following observations. Although the individual parameters A_{CC} and A_{HH} are different,[54] the total atom–atom interaction for the dispersion energy is in remarkably good agreement with the *ab initio* result, yielding a nearly constant fraction of 80% of this result for different orientations. The remaining difference of 20% can have several reasons, but it may be due also to the inaccuracy of the *ab initio* result for the dispersion energy, which has been computed in the multipole expansion only (see Sec. II). For the short range repulsions the most striking difference is the longer range (smaller exponent) of the C–C interactions in the *ab initio* calculations ($C_{CC} = 3.16$ Å^{-1}). The empirical exponent of 3.60 Å^{-1} was found from the layer spacing and compressibility of graphite[55] and was fixed while the other parameters, A and B, were empirically optimized.[2] In relation to this *ab initio* result, it is inter-

esting that Williams has observed[2] that the substitution of optimized A and B parameters into the graphite calculation[55] would have yielded an exponent of 3.20 Å^{-1} or 2.94 Å^{-1}. He ascribes this to the "softness" of the π-electron clouds, which is confirmed by our *ab initio* calculations (the fit of C_{CC} on the π-stacked geometries I and II yields a value of 2.95 Å^{-1}). The exponent for the H–H repulsion is in very good agreement. Although the deviation between the theoretical and the empirical atom–atom repulsions is definitely larger than for the dispersion attraction, the strong anisotropy in the short range repulsion is still rather well represented by the empirical potential. The electrostatic interactions are not well represented by the empirical atom–atom potentials. In most empirical parametrizations, e.g., in the first Williams' potential in Table IV, they are simply omitted. In some other parametrizations (the second Williams' potential in our Table IV) they are included, and it has recently been argued[20] that this con-

TABLE IV. Potential parameters.

Parameters		*ab initio* fit ①	empirical ①	empirical ②
B (kcal/mole)	C–C	27116	83630	71461
	C–H	6378	8770	14316
	H–H	1500	2650	2868
C (Å^{-1})	C–C	3.16	3.60	3.60
	C–H	3.43	3.67	3.67
	H–H	3.70	3.74	3.74
A (kcal/mole Å^6)	C–C	876	568	449.3
	C–H	132	125	134.3
	H–H	20	27.3	40.15
q (unit charges)	C	−0.5274[a]	···	−0.24
	H	+0.2637[a]	···	+0.12

[a]With the charges shifted from the nuclei (see Fig. 1); from the fit ② with the charges on the nuclei we find $q_C = -0.3950$, $q_H = +0.1975$.
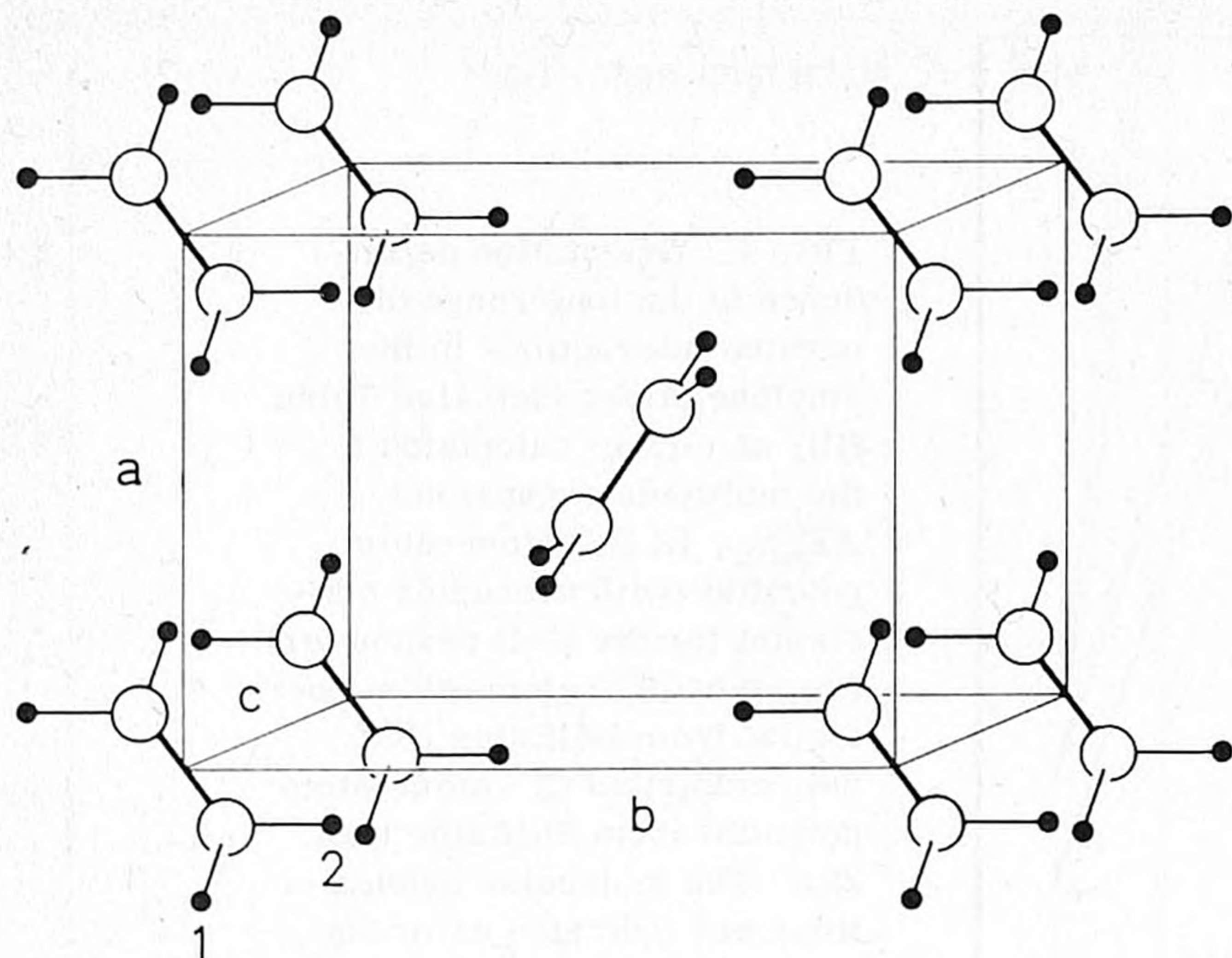
FIG. 5.   Structure of the ethylene crystal, symmetry $P2_1/n$ $(Z = 2)$.

siderably improves the calculated results for the lattice structure and the phonon frequencies. Still, the charges in the empirical models are much smaller than the values from our theoretical atom–atom potential and this will lead to an underestimate of the electrostatic (mainly quadrupole–quadrupole) interaction. Probably, this lack of electrostatic interactions between the molecules is implicitly corrected for by the adjustment of the other empirical parameters.

IV. LATTICE DYNAMICS CALCULATIONS ON THE ETHYLENE CRYSTAL

A. Procedure and results

Before using the intermolecular potential derived from dimer calculations in the crystal we must consider the problem of additivity of the interactions between molecules (which may still hold even if the additivity assumption does not hold for the atom–atom potentials). The electrostatic interactions are exactly pairwise additive. For the exchange interactions between molecules the many-body components are expected to be small[56] because the intermolecular overlap is quite small. For the dispersion forces the most important many-body component is the Axilrod–Teller or triple–dipole energy which is also small compared with the pair energy. [57] The only component in the first and second order interaction energy for which pairwise additivity does not even hold approximately is the induction energy. This energy is already very small in the ethylene dimer, however, relative to the other terms and we can expect it to be even smaller in the crystal, because there each molecule is surrounded by a more symmetric environment. Therefore, we can safely neglect the induction energy in our calculations for the ethylene crystal and assume pairwise additivity for all other interactions.

The precise structure of the ethylene crystal is known only recently from x-ray[58] and neutron[59] diffraction. Both for normal ethylene and for the completely deuterated substance the symmetry group is the monoclinic space group $P2_1/n$ (C_{2h}^5), with two centrosymmetric molecules in the unit cell (Fig. 5). For a long time,

there has been some uncertainty regarding the positions of the hydrogen atoms, i.e., about the rotation of the molecular plane around the C–C axis. From the older x-ray data[60] and simple packing considerations two crystal structures appeared possible, which are both in agreement with the measured ir spectra[61] and which differ only in that the two molecules in the unit cell are tilted in the same or in opposite sense around their C–C axes, thus leading to a screw axis in the a or b direction, respectively. Actually, several lattice dynamics calculations[33–36] with empirical atom–atom potentials were performed in an attempt to settle this problem.

In our lattice dynamics calculations we have assumed the b-structure, which proved to be the correct one.[58,59] As a first step, which is theoretically required[62] but which is often not made in practice, we have optimized the seven structural parameters (the unit cell dimensions a, b, c and the angle β and the angles ξ, η, ζ describing the molecular orientation) for the given potential. This optimization was carried out by minimizing the lattice energy with respect to all seven parameters simultaneously, using the procedures contained in the MINUIT program package[63] (with repeated checks that the minimum obtained was really the absolute one). The lattice sum was taken over 42 neighboring molecules,[64] after checking that the inclusion of further shells did not influence the results anymore (except, slightly, the total cohesion energy). The structural data are listed in Table V. Then, the force constants were evaluated and the dynamical problem was solved in the harmonic approximation:

$$\sum_{\sigma'=1}^{2} \sum_{\beta=1}^{6} [D_{\alpha\beta}^{\sigma\sigma'}(\mathbf{q}) - \omega^2(\mathbf{q}, j) M_{\alpha\beta}\delta_{\sigma\sigma'}] e_{\beta}^{\sigma'}(\mathbf{q}, j) = 0 . \tag{6}$$

The tensor **M** contains the molecular mass ($M_{\alpha\beta} = M\delta_{\alpha\beta}$ for α, $\beta = 1$, 2, 3) and the moments of inertia ($M_{\alpha\beta} = I_{\alpha-3,\beta-3}$ for α, $\beta = 4$, 5, 6). The dynamical matrix is given by:

$$D_{\alpha\beta}^{\sigma\sigma'}(\mathbf{q}) = \sum_{l'} \Phi_{\alpha\beta}\begin{pmatrix} 0 & l' \\ \sigma & \sigma' \end{pmatrix} \exp[-i\mathbf{q} \cdot (\mathbf{R}^0 - \mathbf{R}^{l'})]$$

and the force constants:

$$\Phi_{\alpha\beta}\begin{pmatrix} l & l' \\ \sigma & \sigma' \end{pmatrix} = \left[\frac{\partial^2 V\begin{pmatrix} l & l' \\ \sigma & \sigma' \end{pmatrix}}{\partial u_\alpha^\sigma(l) \, \partial u_\beta^{\sigma'}(l')} \right]_0$$

have been evaluated at the equilibrium positions of the molecules found from the energy minimization. The indices σ, σ' label different sublattices, l, l' label different unit cells, α, $\beta = 1$, 2, 3 denote translational coordinates (x, y, z), α, $\beta = 4$, 5, 6 denote rotational coordinates (θ_x, θ_y, θ_z). The quantities $\omega(\mathbf{q}, j)$ are the phonon frequencies for the given wave vector $\mathbf{q}$ and branch j. All calculations were carried out in an orthogonal fixed frame a, b, c^*. For details of the formalism we refer to the review paper by Venkataraman. [62]

We expect that the effect of anharmonic corrections is not very large for ethylene since the temperature effect on the ir spectra[66] is small (for 10 °K $< T <$ 65 °K). Actually, we have studied this effect in a self-consistent phonon calculation, [67] using an empirical potential. Also

TABLE V. Lattice dynamics of the C_2H_4 crystal.

Potential:		Experiment	Ab initio fit ①[a]		Empirical ○[b]		Empirical ○		Fit ○ with $q=0$[d]		Fit ○[e]		
Unit cell[f]	a(Å)	4.626	4.730		4.856		4.726		4.844		4.763		
	b(Å)	6.620	6.205		6.342		6.435		6.516		5.990		
	c(Å)	4.067	4.005		3.832		4.135		3.886		4.138		
	β(degrees)	94.4	88.5		96.8		94.0		99.0		88.1		
Molecular[f] orientation	ξ(degrees)	−27.0	−31.7		−36.2		−27.0		−34.4		−26.3		
	η(degrees)	−14.6	−9.3		−5.0		−11.7		−7.4		−8.4		
	ζ(degrees)	−34.3	−31.3		−27.8		−31.8		−28.7		−31.8		
Cohesion energy[g] (kcal/mole)	short range	...	−4.84		−3.42		−3.08		−3.88		−4.93		
	dispersion	...	8.89		7.46		6.58		8.16		8.87		
	electrostatic	...	1.41		0.0		0.42		0.0		1.69		
	total	4.7	5.46		4.04		3.92		4.28		5.63		
ir[h] ω(cm⁻¹)		...	$57^{(1.07)}$	$75^{(1.07)}$	$50^{(1.07)}$	$60^{(1.07)}$	$61^{(1.07)}$	$63^{(1.07)}$	$59^{(1.07)}$	$52^{(1.07)}$	$55^{(1.07)}$	$78^{(1.07)}$	Au
		$73^{(1.05)}$	$73^{(1.07)}$	$94^{(1.07)}$	$60^{(1.07)}$	$67^{(1.07)}$	$75^{(1.07)}$	$75^{(1.07)}$	$96^{(1.07)}$	$66^{(1.07)}$	$75^{(1.07)}$	$105^{(1.07)}$	Au
		$110^{(1.06)}$	$94^{(1.07)}$	$126^{(1.07)}$	$90^{(1.07)}$	$115^{(1.07)}$	$108^{(1.07)}$	$113^{(1.07)}$	$132^{(1.07)}$	$111^{(1.07)}$	$93^{(1.07)}$	$132^{(1.07)}$	Bu
Raman[i] ω(cm⁻¹)		$73^{(1.22)}$	$51^{(1.22)}$	$50^{(1.21)}$	$51^{(1.21)}$	$55^{(1.20)}$	$59^{(1.22)}$	$38^{(1.22)}$	$46^{(1.21)}$	$56^{(1.20)}$	$26^{(1.24)}$	imag···	Bg
		$90^{(1.20)}$	$84^{(1.22)}$	$80^{(1.19)}$	$74^{(1.18)}$	$87^{(1.17)}$	$89^{(1.19)}$	$79^{(1.21)}$	$23^{(1.24)}$	$76^{(1.18)}$	$72^{(1.22)}$	$85^{(1.18)}$	Ag
		$97^{(1.24)}$	$87^{(1.17)}$	$105^{(1.20)}$	$83^{(1.21)}$	$100^{(1.21)}$	$94^{(1.20)}$	$90^{(1.18)}$	$89^{(1.20)}$	$82^{(1.21)}$	$88^{(1.18)}$	$93^{(1.20)}$	Ag
		$114^{(1.20)}$	$131^{(1.18)}$	$157^{(1.17)}$	$102^{(1.17)}$	$114^{(1.18)}$	$128^{(1.18)}$	$131^{(1.18)}$	$99^{(1.33)}$	$103^{(1.18)}$	$128^{(1.21)}$	$168^{(1.19)}$	Bg
		$167^{(1.36)}$	$181^{(1.41)}$	$196^{(1.41)}$	$156^{(1.40)}$	$183^{(1.41)}$	$1.75^{(1.40)}$	$163^{(1.40)}$	$139^{(1.35)}$	$140^{(1.41)}$	$178^{(1.40)}$	$164^{(1.19)}$	Ag
		$177^{(1.31)}$	$211^{(1.40)}$	$249^{(1.41)}$	$139^{(1.41)}$	$193^{(1.41)}$	$1.71^{(1.40)}$	$170^{(1.41)}$	$144^{(1.25)}$	$142^{(1.41)}$	$200^{(1.36)}$	$220^{(1.39)}$	Bg

[a]Best atom−atom fit to the ab initio potential.

[b]From Williams (Ref. 28).

[c]From Williams (Ref. 29).

[d]Potential from ab initio fit ① with the electrostatic (point charge) term omitted.

[e]Atom−atom fit with the point charges on the nuclei.

[f]Experimental results from Ref. 58 at $T=85$ °K. The angles ξ, η, ζ describing the molecular orientation are defined as follows: Start with the molecule lying in the ac* plane, the C−C axis along the a axis, and rotate by ξ, η, ζ about the a, b, and c^* axes, respectively.

[g]Experimental result from Ref. 69, corrected for the zero point vibrational energy (0.5 kcal/mole, from Ref. 67).

[h]Experimental frequencies from Ref. 66 at $T=20$ °K.

[i]Experimental frequencies from Ref. 35 at $T=30$ °K. The number in parentheses denotes the isotope ratio $\omega_{C_2H_4}/\omega_{C_2D_4}$. The calculated frequencies in the first column have been obtained from the dynamical matrix at the experimental geometry, those in the second column at the equilibrium geometry for the given potential (Except for the fit ① with $q=0$, where the first column was calculated at the equilibrium geometry for the full fit ○ potential).
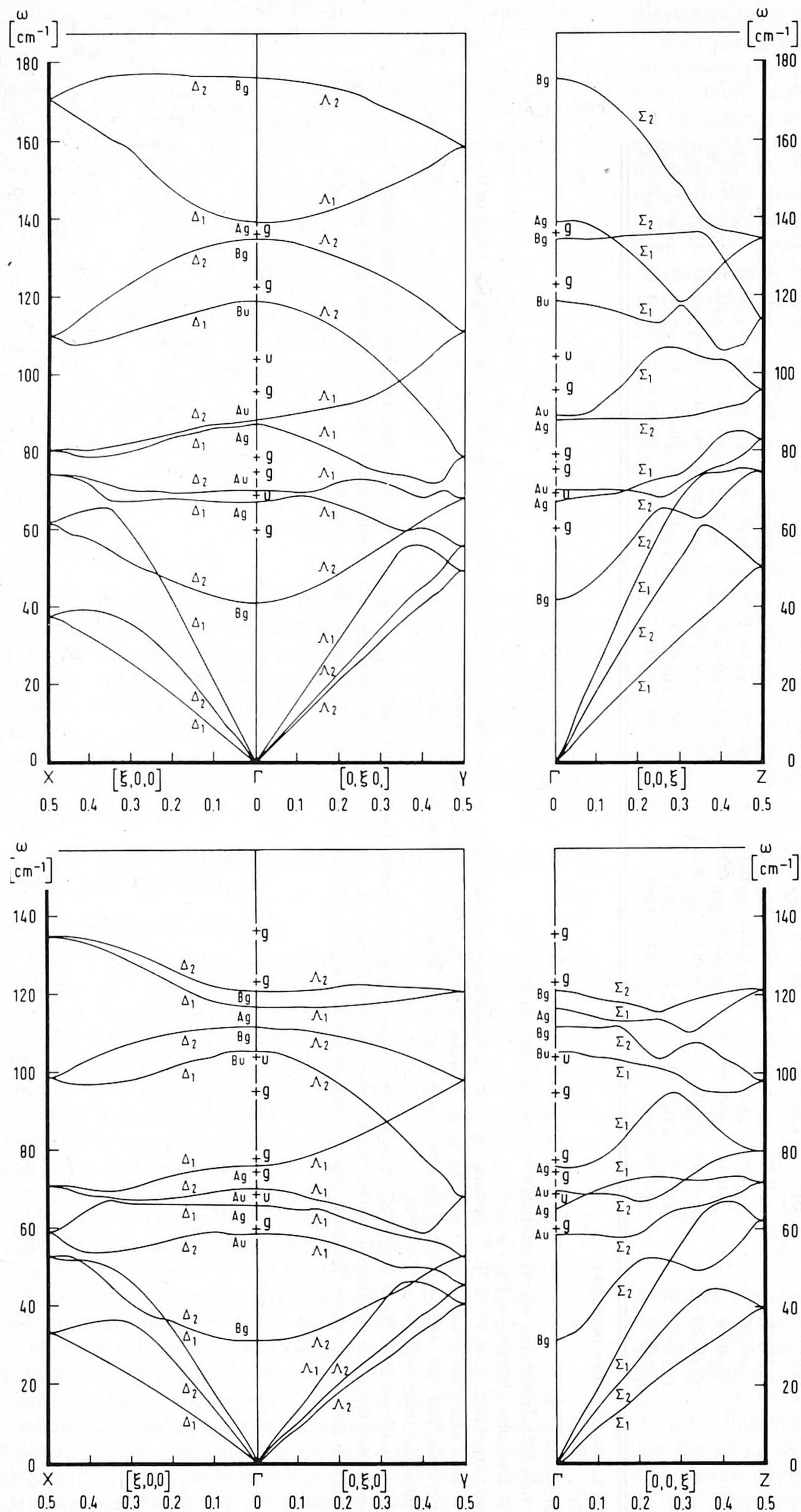
FIG. 6. Phonon dispersion curves in C_2D_4 for q along the X ($=a*$), Y ($=b*=b$) and Z ($=c*$) directions in the ethylene crystal; a. Calculated with the *ab initio* atom–atom potential, fit ①, and b. Calculated with the atom–atom potential, empirical ② from Williams (Ref. 29). For each potential the crystal structure is relaxed to equilibrium (within the given symmetry) before calculating the dynamical matrix. The crosses at the Γ-point ($q=0$) indicate the experimental results from ir (u) and Raman (g) spectroscopy.

the other approximation which is inherent in the present formalism, the rigid molecule approximation, is expected to hold rather well for ethylene since the lowest internal vibration mode lies at a frequency of 810 cm^{-1},[35] far above the lattice modes.

We have performed the calculation of the ir and Raman frequencies $\omega(q=0)$ both for normal C_2H_4 and for C_2D_4 in order to look at the isotopic shifts in the Raman spectrum; the phonon dispersion curves have been calculated for C_2D_4 (Fig. 6) since inelastic neutron scat-

tering experiments can be expected in the near future.[68] For comparison with other lattice dynamics calculations on ethylene which have not optimized the structure parameters for the atom–atom potential used, we have also performed some calculations of the phonon frequencies in the experimental[58] structure.

The results for the theoretical atom–atom potential are listed in Table V, together with the results for the two empirical Williams potentials from Table IV. Since these empirical potentials neglect or undervalue the effect of the electrostatic forces, we have studied the effect of these forces by performing a calculation with the theoretical atom–atom potential without the electrostatic (point charge) interactions (with or without reoptimizing the crystal structure). Also we have carried out phonon calculations using the theoretical potential with the atomic charges centered on the nuclei.

B. Conclusions

The structure of the ethylene crystal calculated with the interaction potential from *ab initio* calculations is in rather good agreement with the experimental structure.[58] The lattice cohesion energy is just slightly too high.[69] The frequencies of the lattice modes agree reasonably well with the ir and Raman data.[66,35] Particularly we find, in accordance with the experimentally observed isotope shifts in the Raman frequencies that the two highest frequency modes correspond with librations of the molecules around their C–C axes.

The theoretical model potential with the atomic charges centered on the nuclei, besides making a less good fit to the *ab initio* electrostatic interaction, also behaves considerably worse in the lattice calculations.

When comparing with the results for the empirical potentials we observe that the latter are still giving better crystal properties, especially the second Williams potential which comprises an electrostatic term. We must keep in mind, however, that part of these properties (the structure and the cohesion energy for a series of related hydrocarbons), have actually been used for parametrizing these potentials, whereas the other properties, the phonon frequencies, are strongly related with the criterion used for optimizing the empirical parameters[30] (the minimization of the forces on the molecules for the experimental crystal structure). The latter relation is confirmed by Williams' recent conclusion[30] that the inclusion of the phonon frequencies in the parametrization of the empirical atom–atom potentials hardly changes the potential obtained from the static crystal properties. The *ab initio* potential has not been adapted to any empirical data and, therefore, we can consider the agreement with the experimental crystal properties as very satisfactory.

The omission of the electrostatic (point charge) interactions from the *ab initio* potential has a distinct (lowering) effect on the phonon frequencies, in particular for the higher librational modes. This is quite understandable in view of the strong orientational dependence of these interactions. It is typical that the empirical potentials which underestimate or even neglect these (mainly molecular quadrupole–quadrupole) interactions still yield the correct magnitude for the phonon frequencies. This could be caused by a slight adaptation of the empirical parameters in the short range repulsions. If such potentials are used for the calculation of (macroscopic) properties which are dependent on the long range anisotropy of the interactions between the molecules this could lead to serious errors.

While we have found that the empirical potentials are in reasonable agreement with the *ab initio* calculations, except for the electrostatic contribution, we can also conclude that further parameter optimization of the (empirical) atom–atom potentials for the hydrocarbons, taking into account even more experimental solid state data, is probably not meaningful. We think on the basis of our *ab initio* results that remaining discrepancies between calculated and experimental crystal properties are due to the deficiencies of the atom–atom model. Possibly the use of other data, from beam scattering, relaxation measurements or Van der Waals molecules, could support our conclusions about the importance of electrostatic interactions.

[1]A. I. Kitaigorodski, *Molecular Crystals and Molecules*, (Academic, New York, 1973).
[2]D. E. Williams, J. Chem. Phys. 45, 3770 (1966).
[3]D. E. Williams, Acta Cryst. A 30, 71 (1974).
[4]A. T. Hagler and S. Lifson, Acta Cryst. B 30, 1336 (1974).
[5]T. Luty and G. S. Pawley, Chem. Phys. Lett. 28, 593 (1974).
[6]R. P. Rinaldi and G. S. Pawley, J. Phys. C 8, 599 (1975).
[7]A first test for the long range interactions has been made in Ref. (8). The results have been included in the discussion in this paper.
[8]F. Mulder and C. Huiszoon, Mol. Phys. 34, 1215 (1977).
[9]M. Faubel and J. P. Toennies, Advan. At. Mol. Phys. 13, 229 (1978).
[10]J. Reuss, Advan. Chem. Phys. 30, 389 (1975).
[11]R. Schafer and R. G. Gordon, J. Chem. Phys. 58, 5422 (1973).
[12]R. J. LeRoy and J. van Kranendonk, J. Chem. Phys. 61, 4750 (1974).
[13]S. E. Novick, S. S. Harris, K. C. Janda, and W. Klemperer, Can. J. Phys. 53, 2007 (1975).
[14]V. Magnasco and G. F. Musso, J. Chem. Phys. 48, 2657 (1968).
[15]G. Tapia, G. Bessis, and S. Bratos, Int. J. Quantum Chem. S4, 289 (1971).
[16]C. F. Bender and H. F. Schaefer, J. Chem. Phys. 57, 217 (1972).
[17]M. Jazunski, E. Kochanski, and P. Siegbahn, Mol. Phys. 33, 139 (1977).
[18]G. A. Gallup, Mol. Phys. 33, 943 (1977).
[19]W. Meyer, Chem. Phys. 17, 27 (1976).
[20]F. Mulder, A. van der Avoird and P. E. S. Wormer, Mol. Phys. (in press).
[21]M. Kraus and F. M. Mies, J. Chem. Phys. 42, 2703 (1965).
[22]M. D. Gordon and D. Secrest, J. Chem. Phys. 52, 120 (1970).

[23]B. Tsapline and W. Kutzelnigg, Chem. Phys. Lett. **23**, 173 (1973).

[24]P. J. M. Geurts, P. E. S. Wormer, and A. van der Avoird, Chem. Phys. Lett. **35**, 444 (1975).

[25]P. C. Hariharan and W. Kutzelnigg, Progress Report Lehrstuhl für Theoretische Chemie, Ruhr Universität Bochum Fed. Republic of Germany (1977).

[26]R. D. Etters, R. Danilowicz, and W. England, Phys. Rev. A **12**, 2199 (1975).

[27]J. F. Silvera and V. V. Goldman (to be published).

[28]D. E. Williams, J. Chem. Phys. **47**, 4680 (1967).

[29]D. Hall and D. E. Williams, Acta Cryst. A **31**, 56 (1975).

[30]T. L. Starr and D. E. Williams, Acta Cryst. A **33**, 771 (1977).

[31]A. Warshell and S. Lifson, J. Chem. Phys. **53**, 582 (1970).

[32]G. Fillipini, C. M. Gramaccioli, M. Simonetta, and G. B. Suffritti, J. Chem. Phys. **59**, 5088 (1973).

[33]D. A. Dows, J. Chem. Phys. **36**, 2836 (1967).

[34]G. Taddei and E. Giglio, J. Chem. Phys. **53**, 2768 (1970).

[35]G. R. Elliot and G. E. Leroi, J. Chem. Phys. **59**, 1217 (1973).

[36]F. Vovelle and G. G. Dumas, C. R. Acad. Sci. Ser. B **281**, 239 (1975).

[37]M. Hashimoto, M. Hashimoto, and T. Isobe, Bull. Chem. Soc. Jpn. **44**, 3230 (1971).

[38]P. E. S. Wormer and A. van der Avoird, J. Chem. Phys. **62**, 3326 (1975).

[39]F. Mulder, M. van Hemert, P. E. S. Wormer, and A. van der Avoird, Theoret. Chim. Acta **46**, 39 (1977).

[40]P. E. S. Wormer, F. Mulder, and A. van der Avoird, Int. J. Quantum Chem. **11**, 959 (1977).

[41]P. H. Smit, J. L. Derissen, and F. B. van Duijneveldt, Mol. Phys. (in press).

[42]P. H. Smit, Ph. D. thesis, Utrecht, 1978.

[43]Using the program COULEX written by P. E. S. Wormer, Nijmegen, 1976.

[44]P. E. S. Wormer, unpublished results.

[45]F. Mulder, unpublished results.

[46]N. J. Bridge and A. D. Buckingham, Proc. Roy. Soc. A **295**, 334 (1966).

[47]G. W. Hills and W. J. Jones, J. Chem. Soc. Faraday Trans. II **71**, 812 (1975).

[48]L. W. Flynn and G. Todos, Am. Inst. Chem. Eng. **8**, 362 (1962).

[49]A. D. King, J. Chem. Phys. **51**, 1262 (1969).

[50]It should be noted here that we have also considered other solutions for correcting $\Delta E^{(1)}_{\text{point charge}}$ for penetration effects, such as the use of screened point charge interactions. This model fails in representing the exact penetration interactions, however, which are attractive for all molecular orientations due to the incomplete screening of the nuclei with respect to the electrons (except for very small R, where the nuclear repulsions dominate).

[51]F. Mulder, P. J. M. Geurts, and A. van der Avoird, Chem. Phys. Lett. **33**, 215 (1975).

[52]A. van der Avoird and P. E. S. Wormer, Mol. Phys. **33**, 1367 (1977).

[53]L. Salem, Proc. Royal Soc. A **264**, 379 (1961).

[54]This difference would have been reduced if we had used foreshortened C–H bond lengths[30] in fitting the *ab initio* results.

[55]A. D. Crowell, J. Chem. Phys. **29**, 446 (1958).

[56]R. F. W. Bader, O. A. Novaro, and V. Beltran-Lopez, Chem. Phys. Lett. **8**, 568 (1971).

[57]H. Margenau and N. R. Kestner, *The Theory of Intermolecular Forces*, (Pergamon, Oxford, 1969), p. 151.

[58]G. J. H. van Nes and A. Vos, Acta Cryst. B **33**, 1653 (1977).

[59]W. Press and J. J. Eckert, J. Chem. Phys. **65**, 4362 (1976).

[60]C. W. Bunn, Trans. Faraday Soc. **40**, 23 (1944).

[61]C. Brecher and R. S. Halford, J. Chem. Phys. **35**, 1109 (1961).

[62]G. Venkataraman and V. S. Sahni, Rev. Mod. Phys. **42**, 409 (1970).

[63]CERN Computer Centre Program Library, D 506, D 516, F. James and M. Roos, authors.

[64]The separation of molecules into parts, when truncating the lattice sum of the atom–atom interactions[65] should be avoided since this makes the electrostatic interactions fall off with R^{-1}, whereas the leading term is R^{-5} (quadrupole–quadrupole) when whole molecules are considered.

[65]D. E. Williams and T. L. Starr, Comput. Chem. **1**, 173 (1977).

[66]M. Brith and A. Ron, J. Chem. Phys. **50**, 3053 (1969).

[67]T. Wasiutynski, in: Proceedings of the Lattice Dynamics Conference, edited by M. Balkanski, (Flammarion, Paris 1977).

[68]U. Buchenau, Jülich, private communication.

[69]C. J. Egan and J. D. Kemp, J. Am. Chem. Soc. **59**, 1264 (1937).